Phase Behavior of Polymer–Supercritical Chlorodifluoromethane Solutions

Charles W. Haschets and Annette D. Shine*

Department of Chemical Engineering, University of Delaware, Newark, Delaware 19716

Received March 12, 1993; Revised Manuscript Received June 11, 1993[●]

ABSTRACT: The phase behavior of solutions of poly(methyl methacrylate) and polycaprolactone (PCL) in supercritical chlorodifluoromethane (CDFM) has been studied experimentally using a high-pressure variable-volume view cell; LCST phase behavior was observed. The P–x and T–x demixing curves were generally flat up to the maximum concentration studied of 19 wt % polymer. The Sanchez–Lacombe lattice fluid (LF) model was fit to the experimental data as well as to previously published data for polyethylene (PE)–propane and polyethylene–n-pentane mixtures. The LF model predicted LCST phase behavior in all cases. Without using adjustable mixing rule parameters, the LF model significantly overpredicted the demixing pressures and the slope of the demixing curves. The Panayiotou–Sanchez hydrogen bond model without LF parameters provided a somewhat improved description of the magnitude of the demixing pressures for the CDFM solutions but could not describe the experimental maximum pressure. Over a temperature range of 70–140 °C, the experimental maximum pressure for the polymer–CDFM isotherms were fit using a single set of LF mixing rule parameters for each solution. Correct scaling of molecular weight was found for the PCL–CDFM and the PE–n-alkane solutions.

Introduction

Supercritical fluids (SCFs) have recently been used in a variety of conventional polymer processes such as fractionation[1,2] and swelling[3,4] as well as in the development of innovative technologies.[5–9] SCF solvents are an attractive alternative to incompressible liquid solvents due to the special characteristics of SCFs, which can have the density and dissolving power of a liquid while exhibiting transport properties of a gas. Phase behavior data for polymer–supercritical fluid systems are desired to optimize existing processes or to develop new ones, yet relatively few studies of polymer/SCF phase behavior have been reported to date.

Carbon dioxide is often used in SCF processes because it has a low critical temperature and pressure and because it is nonflammable, nontoxic, and inexpensive. However, it is generally a poor solvent for both polar and nonpolar high molecular weight polymers, although oligomers can be soluble in supercritical carbon dioxide.[10] Hydrocarbon solvents[11–21] and hydrochlorofluorocarbons (HCFCs),[1,22,23] on the other hand, have been shown to be good solvents for a variety of high molecular weight polymers.

For example, Ehrlich and co-workers[17,19] have studied the phase behavior of polyethylene (PE) in near-critical and supercritical n-alkanes. In their study of PE of molecular weights from 13 600 to 120 000 in n-propane, it was inconclusive if the experimental data exhibited upper consolute solution temperature (UCST) or lower consolute solution temperature (LCST) phase behavior due to the flatness of the cloud point curves. The demixing isotherms were relatively flat over the concentration range studied, 0.25–10 wt % and the demixing pressures only varied by about 25% between the lowest and highest molecular weight isotherms. Others have observed similar phase behavior for polyethylene in n-alkanes[14] as well as in ethylene.[18,24–26]

Kiran and co-workers[11–13] have studied the phase behavior of low molecular weight polystyrene in supercritical n-alkanes and observed UCST phase behavior. The demixing curves for 4000 and 9000 molecular weight PS in n-butane were relatively flat throughout the entire composition range studied (1–80 wt %) except at the lowest and highest concentrations. Demixing pressures doubled in magnitude upon increasing the molecular weight from 4000 to 9000. For polyethylene of molecular weights from 2100 to 420 000, Kiran and Zhuang[14] observed LCST phase behavior in high-pressure n-pentane. The demixing curves were also relatively flat over the concentration range studied (0.05–15 wt %), while demixing pressures only increased by about 25% from the lowest to highest molecular weight cases.

The phase behavior of polyisobutene with molecular weights ranging from 1170 to 2 250 000 in n-pentane was studied by Allen and Baker.[16] Relatively flat LCST curves were found for concentrations up to about 20 wt %, with a steeper temperature dependence exhibited for concentrations greater than about 20 wt %. Increasing the molecular weight by 2 orders of magnitude only lowered the demixing curves by about 60 °C.

Meilchen et al.[1] have recently reported the phase behavior of acrylate polymers in supercritical chlorodifluoromethane (CDFM) and propane. They observed that high acrylate content polymers were virtually insoluble in nonpolar propane but were soluble in CDFM. The solubility in CDFM was attributed to hydrogen bonding with the acrylate group. Other ester-containing polymers were found soluble in CDFM by Lele and Shine[5] at conditions both below and above the critical point of the solvent, up to pressures of 40 MPa and temperatures of 160 °C. They concluded that the solvent power of CDFM increased with increasing density and that polymer solubility was negligible below a solvent density of 880 kg/m^3.

Most of the polymer–SCF systems experimentally studied have been low molecular weight polymers or oligomers, while few data exist for high molecular weight systems. In general, polymer–SCF solvent systems usually exhibit LCST phase behavior for high molecular weight polymers, while low molecular weight systems usually exhibit a UCST. In both cases, the demixing curves are relatively flat. For high molecular weight polymers, there is typically only a 10–25% increase in the magnitude of the demixing pressures upon doubling the molecular weight.

[●] Abstract published in *Advance ACS Abstracts*, August 15, 1993.

0024-9297/93/2226-5052$04.00/0

Table I. Properties of Polymers

polymer	M_w	M_n	T_g, °C
poly(methyl methacrylate)	74200[a]	70000[a]	125
polycaprolactone	14 600	9300	−60
polycaprolactone	40500	26400	−60

[a] Reported by supplier.

In order to design SCF–polymer processes without resorting to extensive and expensive experimental characterization, it is desirable to obtain a complete theoretical model that accurately predicts the experimental phase behavior of polymer–SCF solutions. For the polymer–CDFM systems of interest in this study, a theory must describe LCST phase behavior and account for significant compressibility effects and specific interactions such as hydrogen bonding. The Sanchez–Lacombe[27] and the Panayiotou–Sanchez[28] models have been used previously to predict the phase behavior of polymer–liquid solvent systems but have not been extensively tested for polymer–SCF solvent systems exhibiting LLE phase behavior. However, Meilchen et al.[1] have modeled experimental poly(methyl acrylate) in CDFM and poly(ethylene-*co*-methyl acrylate) copolymers in CDFM and in propane using the LF model. Temperature-dependent parameters were needed to describe the experimental cloud point data. Also, Gupta et al.[29] have used the HB model to study the extent of hydrogen bonding in supercritical fluids such as pure alcohols and water. Neither the LF nor the HB model has been extensively used to describe high molecular weight polymer–SCF systems that exhibit hydrogen bonding such as those in our study.

In this study, the phase behavior of poly(methyl methacrylate) and polycaprolactone in chlorodifluoromethane was determined experimentally using a high-pressure variable-volume view cell. The effect of polymer polydispersity and the critical state of the solvent on the phase behavior was examined. The ability of the Sanchez–Lacombe lattice fluid and the Panayiotou–Sanchez hydrogen bond models to describe our experimental data was investigated, as was the suitability of the LF model in describing the nonpolar binary mixtures studied by Condo et al.[19] and Kiran and Zhuang.[14]

Experimental Section

The phase behavior of poly(methyl methacrylate) (PMMA) and polycaprolactone (PCL) in chlorodifluoromethane (CDFM) was determined with a high-pressure variable-volume view cell. Characteristics of the polymers used are shown in Table I.

The monodisperse ($M_w/M_n \approx 1.06$) PMMA was synthesized by Dr. Steven Smith of the Procter & Gamble Co. via group transfer polymerization. It had 57% syndiotactic triads, 37% heterotactic triads, and 6% isotactic triads, which is similar to that of conventional free radical PMMA. Both PCLs were obtained from Union Carbide Corp. and had polydispersities of approximately 1.6. The PCL molecular weight was measured by gel permeation chromatography using the universal calibration based on PCL standards. The polymer T_gs were determined using differential scanning calorimetry. The critical properties of CDFM (Freon 22, Du Pont Co.) are $T_c = 96.3$ °C, $P_c = 4.988$ MPa, and $\rho_c = 514$ kg/m^3 and the liquid density of CDFM at it normal boiling point is 1416 kg/m^3.[30] Neither of the polymers was soluble in carbon dioxide.

The cloud point experiments were performed using the apparatus shown in Figure 1. The system is similar to that used by Meilchen et al.[1] with slight differences in the method of pressure and temperature measurement and control. Known amounts of polymer and solvent were gravimetrically charged to the high-pressure variable-volume view cell (McHugh, Baltimore, MD; pressure rating = 110.3 MPa at 150 °C, internal working volume = 34.2 ± 0.2 cm^3), and the system was pressurized at a fixed temperature by displacing the piston with water using a high-pressure generator (HIP Inc.) to conditions where the polymer dissolved in the solvent. The system pressure was measured on the solvent side of the piston using a Heise gauge with an accuracy of 0.07% of the total pressure span. The temperature of the system was controlled by two ceramic band heaters in series (Industrial Heater Co., Inc., and Instruments and Thermal Products, Inc.) regulated by a temperature controller (Instruments and Thermal Products, Inc.) and was measured to an accuracy of ±0.2 °C using a thermocouple located directly in the interior of the cell. The contents of the cell were mixed with a stirring bar activated by a magnet attached to a variable-speed motor located directly below the cell.

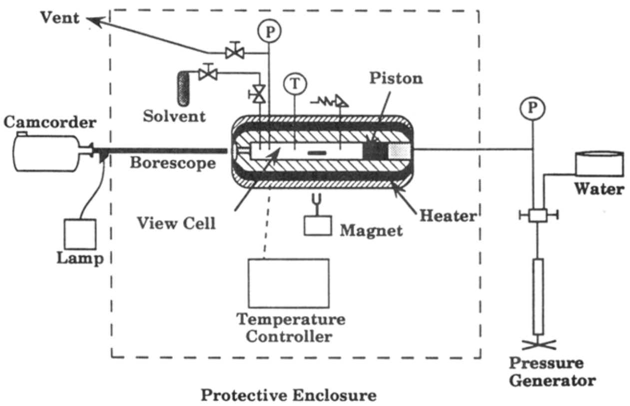

Figure 1. High-pressure phase equilibrium apparatus.

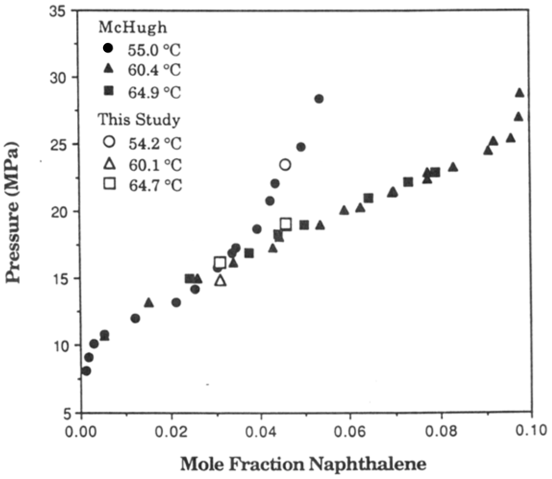

Figure 2. Carbon dioxide–naphthalene solubility comparison. Open symbols are data from this study; closed symbols are from McHugh.[31]

Once thermal equilibrium was achieved, the pressure of the system was slowly decreased at constant temperature until phase separation occurred. The cloud point was visually observed through the sapphire window using a borescope to project the interior of the cell onto a video monitor. The cloud point was defined as the conditions at which the phase separation was initially observed. Using this procedure, cloud point curves for the polymer–CDFM systems were obtained over a temperature range of 50–150 °C. Others have reported the cloud point as conditions of complete turbidity;[1] in this work the incipient and the turbidity definitions for the cloud point pressures varied by at most 0.75 MPa.

Accuracy of the experimental procedure was established by studying the system of naphthalene (Aldrich) in carbon dioxide ("bone dry", Matheson). Figure 2 shows the cloud point pressures obtained from the view cell at 54.2, 60.1, and 64.7 °C in comparison with experimental data of McHugh[31] that were obtained using a flow system with an experimental error of about ±3%. The cloud point pressures obtained from the view cell were in excellent agreement with McHugh's data for all three temperatures, showing that equilibrium data were obtained from the view cell.

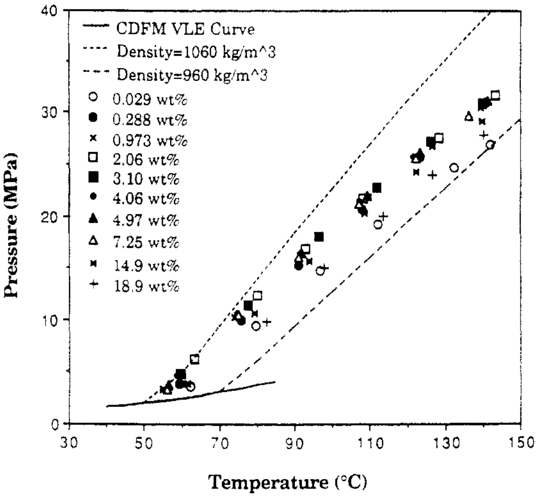

Figure 3. PCL–CDFM cloud point curves (M_w = 14 600). Constant density lines and CDFM VLE curve were calculated from the equation of state of Altunin.[30]

These results, as well as the polymer–CDFM cloud points, were reproducible within 2%.

Experimental Results

Cloud point curves for the 14 600 molecular weight polycaprolactone in CDFM are shown in Figure 3 for polymer concentrations of 0.03–19 wt %. The cloud point pressures for the various concentrations differed by at most 5 MPa, and the isopleths had similar slopes over a temperature range of 55 to about 100 °C. As the temperature was increased above the critical temperature, the lowest and highest isopleths diverged. For example, at 110 °C the could point pressures varied by about 3.5 MPa for all concentrations studied while a 4.5-MPa pressure difference was observed at 140 °C. The intermediate concentration curves were, however, relatively parallel throughout the temperature range. The solvating power of CDFM was decreased as the temperature of the system was increased; i.e., as the temperature was increased, a higher pressure was needed to transform from a two-phase to a one-phase region, so the binary exhibits LCST behavior.

Lines of constant solvent density, calculated from the virial equation of state of Altunin,[30] are included in Figure 3. The cloud point curves did not correspond to lines of constant density but spanned a fairly narrow density range. The upper density limit which separates the one-phase and two-phase regions was about 1060 kg/m^3. Above a solvent density of 1060 kg/m^3, PCL was completely soluble in CDFM for the concentrations studied. Below a density of about 960 kg/m^3, the PCL–CDFM solutions exhibited two phases at all concentrations studied. Thus, a slight decrease in solvent density from 1060 to 960 kg/m^3 would cause phase separation of the PCL and CDFM under any of the conditions examined experimentally.

The cloud point curves for the 40 500 molecular weight polycaprolactone–CDFM system are shown in Figure 4 for concentrations of 0.03–7.24 wt %. The cloud point curves were similar in shape to those of the 14 600 PCL. The effect of increasing the molecular weight from 14 600 to 40 500 only resulted in an increase of the cloud point curves by about 3–5 MPa. The 40 500 PCL was less soluble in CDFM than the lower molecular weight sample, as a higher solvent density was needed to dissolve the 40 500 PCL compared to the 14 600 PCL at the same concentration.

Cloud point curves for the monodisperse PMMA at concentrations from 0.03 to 15 wt % in CDFM are shown in Figure 5. These curves had similar slopes to those observed for the PCL–CDFM systems; however, PMMA more readily dissolved in CDFM than did either PCL, in spite of the higher molecular weight of PMMA.

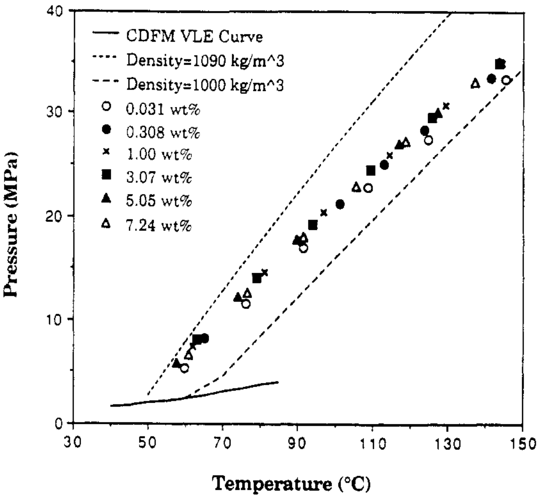

Figure 4. PCL–CDFM cloud point curves (M_w = 40 500). Lines calculated as in Figure 3.

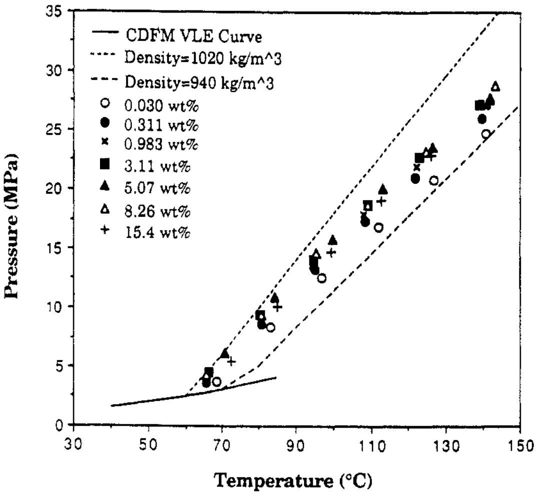

Figure 5. PMMA–CDFM cloud point curves (M_w = 74 200). Lines calculated as in Figure 3.

Also shown in Figures 3–5 is the vapor pressure curve for the pure solvent. The intersection of the saturation curve and the cloud point curves occurred at about 50–55 °C and 2 MPA. This is the lower critical end point of the system. These conditions were in agreement with experimental measurement. At temperatures below 55 °C, a cloud point was not observed upon pressure reduction from a one-phase region. The pressure of the system remained constant at the vapor pressure of the solvent in the one-phase region without further decrease.

The differences in the cloud point curves for the polymer–CDFM systems are more easily seen by examining the pressure–composition and temperature–composition diagrams of each system. P–x profiles were obtained by fitting the CPCs in Figures 3–5 with a second-order polynomial curve to determine the cloud point pressure as a function of temperature (see Appendix for polynomial equations). The pressure was determined from the curve fit for a desired temperature and composition. Several isotherms for the three polymer–CDFM systems are shown in Figures 6–8.

As seen in Figures 6 and 7, the coexistence curves are similar in shape for two molecular weight PCL–CDFM systems for isotherms both above (110 and 140 °C) and below (70 °C) the critical temperature of the solvent. Notice

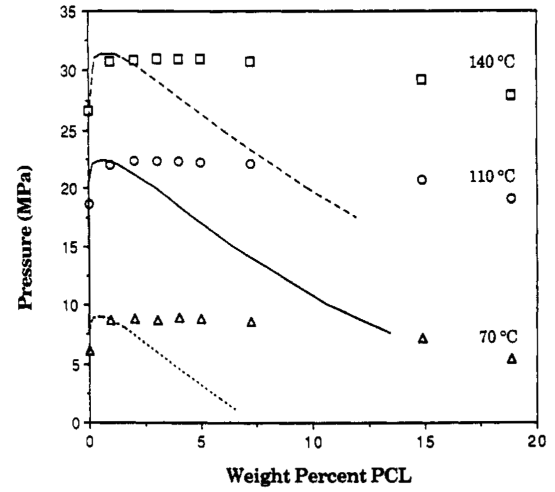

Figure 6. PCL–CDFM pressure–composition curves (M_w = 14 600). Symbols are experimental data; curves were calculated using the LF model with ζ = 1.110 and δ = 0.2068.

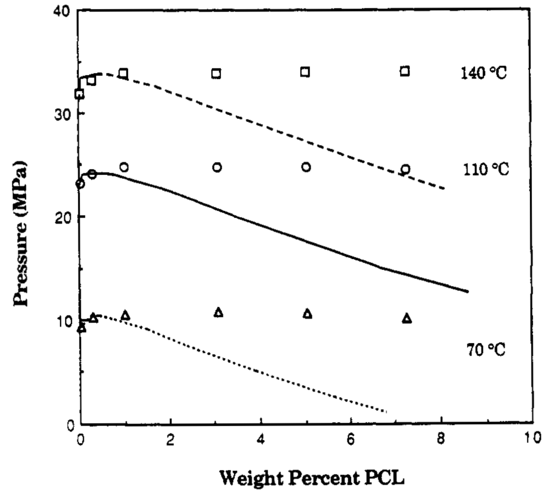

Figure 7. PCL–CDFM pressure–composition curves (M_w = 40 500). Symbols are experimental data; curves were calculated using the LF model with ζ = 1.110 and δ = 0.2068.

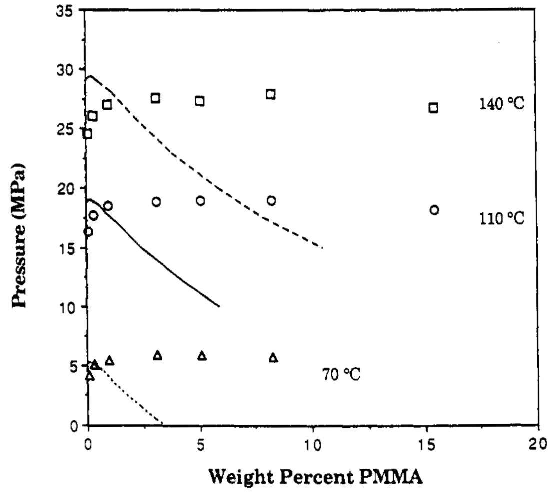

Figure 8. PMMA–CDFM pressure–composition curves (M_w = 74 200). Symbols are experimental data; curves were calculated using the LF model with ζ = 0.980 and δ = 0.5983.

that a 2.5-fold increase in the PCL molecular weight from 14 600 to 40 500 only increased the cloud point pressure by about 10–20%. Similar results were observed for monodisperse polystyrene standards (PS) in dichlorotrifluoroethane (Du Pont, Freon 123) for polymer molecular weights of 114 200 and 929 000.[23] In this case, increasing the PS molecular weight by an order of magnitude only increased the demixing pressures by a factor of 2, similar to the observations of Condo et al.,[19] Kiran and Zhuang,[14] and Allen and Baker[16] for high molecular weight polymers in n-alkanes.

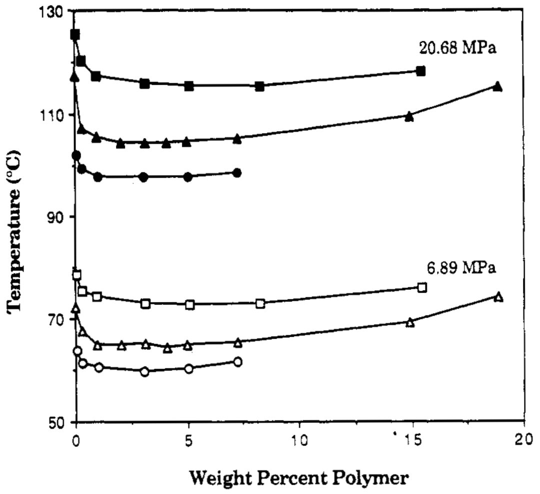

Figure 9. Polymer–CDFM temperature–composition curves: (□) PMMA; (△) 14 600 PCL; (○) 40 500 PCL; closed symbols, 20.68 MPa; open symbols, 6.89 MPa. Lines connect experimental points.

The two different molecular weight PCL isotherms were relatively flat, especially around the critical concentration. The critical concentrations were not experimentally determined, but were approximately 2–5 wt % as seen in Figures 6 and 7. The flatness of the demixing curves follows the trend observed by other workers for polymer–SCF systems.[11-14,17,19,23,26]

Several temperature–concentration isobars (T–x curves) for the two molecular weight PCL–CDFM systems are shown in Figure 9. The usual LCST phase behavior as seen in high molecular weight polymer–SCF solvent systems was observed. LCST behavior in polymer–liquid solvent binaries occurs due to the difference in thermal expansion coefficients (or equivalently, in compressibility or free volume) between the polymer and solvent.[32-34] Since a solvent near or above its critical point is much more compressible than is the polymer solute, LCST behavior is expected to be much more common in polymer–SCF binaries than in polymer–liquid solvent binaries. All polymer–CDFM solutions in this study exhibited LCST behavior.

The T–x curves were also relatively flat over the composition range studied. The PCL demixing temperatures were, however, not very sensitive to the polymer molecular weight. Increasing the molecular weight from 14 600 to 40 500 resulted in lowering the curves by about 10 °C.

The P–x and T–x curves for the monodisperse PMMA–CDFM system are shown in Figures 8 and 9. The demixing pressure and temperature curves for the PMMA–CDFM system exhibited similar shape and flatness near the critical concentration as compared to the two molecular weight PCL systems. Similar behavior was observed for the demixing curves both above and below the critical conditions of the solvent. Since the PMMA used in this study was monodisperse ($M_w/M_n \approx 1.06$) while the PCL samples were polydisperse, the flat shape of the demixing curves cannot be attributed solely to polydispersity effects.

Modeling

Lattice Fluid Model. The LF model developed by Sanchez and Lacombe[27] accounts for physical interactions in binary mixtures containing polymers. Minimization of

Table II. Pure Component Equation of State Parameters

component	T^*, K	P^*, MPa	ρ^*, kg/m^3
chlorodifluoromethane	355	449	1735
propane[27]	371	314	690
n-pentane[27]	441	310	755
polycaprolactone[35]	570	500	1189
polyethylene[27]	649	425	904
poly(methyl methacrylate)[27]	696	503	1269

the free energy with respect to density yields the equation of state:

$$\tilde{\rho}^2 + \tilde{P} + \tilde{T}\left[\ln(1 - \tilde{\rho}) + \left(1 - \frac{1}{r}\right)\tilde{\rho}\right] = 0 \qquad (1)$$

where $\tilde{\rho}$, $\tilde{P}$, and $\tilde{T}$ are the reduced density, pressure, and temperature, respectively, and are defined as follows:

$$\tilde{T} \equiv T/T^* \qquad T^* \equiv \epsilon^*/k$$

$$\tilde{P} \equiv P/P^* \qquad P^* \equiv \epsilon^*/v^*$$

$$\tilde{\rho} \equiv \rho/\rho^* \qquad \rho^* = M/rv^* \qquad (2)$$

Here, T^*, P^*, and ρ^* are the characteristic temperature, pressure, and density, ϵ^* is the mer–mer interaction energy, v^* is the close-packed mer volume, k is the Boltzmann constant, M is the molecular weight, and r is the number of sites (mers) a molecule occupies in the lattice.

The pure component is characterized by three equation of state scaling parameters, T^*, P^*, and ρ^*, or by the three molecular parameters, ϵ^*, v^*, and r. The parameters used for the polymers and solvents are shown in Table II. The parameters for CDFM were found by minimizing the differences in saturation free energy data over a range of 233.15–364.15 K using the procedure suggested by Sanchez and Lacombe.[36] The parameters found were similar to the values determined by Meilchen et al.,[1] which were fit by minimizing the differences between saturation pressures.

The lattice fluid theory is extended to mixtures with the use of appropriate mixing rules. The close-packed volume of the mixture is defined in terms of the pure component volumes as[37]

$$v^* = \phi_1{}^2 v_1{}^* + 2\phi_1\phi_2 v_{12} + \phi_2{}^2 v_2{}^* \qquad (3)$$

with

$$v_{12} = (1 + \delta)\frac{v_1 + v_2}{2} \qquad (4)$$

where v_{12} is the specific close-packed volume "cross term" for the two components of the mixture and ϕ_i is the close-packed volume fraction of component i in the mixture. The deviation of the cross term from the average value of the two pure components is accounted for by the adjustable parameter, δ. A value of $\delta = 0$ suggests simple additivity of the pure component volumes, while $\delta > 0$ signifies deviation from simple additivity and that it is more difficult to pack the two pure components in the mixture.

The total interaction energy of the mixture is defined as a function of the pure component energies as[37]

$$\epsilon^* = \frac{\phi_1{}^2 v_1{}^* \epsilon_{11}{}^* + 2\phi_1\phi_2 v_{12}\epsilon_{12} + \phi_2{}^2 v_2{}^* \epsilon_{22}{}^*}{v^*} \qquad (5)$$

where ϵ_{12} is the mer–mer interaction energy between the two pure components in the mixture. The cross term is estimated as the geometric mean of the two pure component values with an adjustable parameter, ζ, to account for deviations from the geometric mean:

$$\epsilon_{12} = \zeta(\epsilon_1\epsilon_2)^{1/2} \qquad (6)$$

A value of ζ greater than unity signifies a larger mixture mer energy than the geometric mean and would be expected for systems exhibiting strong specific interactions such as hydrogen bonding. Thus, the lattice fluid mixture is described by two adjustable parameters, δ and ζ, with $\delta = 0$ and $\zeta = 1$ representing the base case.

Hydrogen Bond Model. The hydrogen bond model accounts for proton donor and proton acceptor groups possible in the system. In the case of the CDFM–polymer systems of this study only cross association occurs. Evidence in the literature suggests that the hydrogen bond is formed between the hydrogen of CDFM and the carbonyl oxygens of PMMA and PCL.[1,38] Hydrogen bonding to the alkoxyl oxygen does not occur due to steric effects,[38] and self-association of CDFM is very weak if it occurs at all. The CDFM molecule thus has one proton donor, and the number of acceptor groups for the polymers used in this study is equal to the number of carbonyl oxygens in each polymer.

The equation of state for the hydrogen bond model is identical in form to eq 2 except that $1/r$ is replaced by $1/\bar{r}$, where $\bar{r}$ is the modified chain length and is defined in terms of the fraction of hydrogen bonds in the system ν_H:

$$\frac{1}{\bar{r}} = \frac{1}{r} - \nu_H \qquad (7)$$

For a one proton donor–one proton acceptor system ν_H is defined as follows:

$$r\nu_H = \frac{x_1 + ax_2 + A - [(x_1 + ax_2 + A)^2 - 4ax_1x_2]^{0.5}}{2} \qquad (8)$$

where a is the number of proton acceptor groups per molecule and A is given in terms of the free energy change associated with hydrogen bond formation:

$$A = \frac{r}{\tilde{\rho}}\exp\left(\frac{E_{11}{}^\circ + PV_{11}{}^\circ - TS_{11}{}^\circ}{RT}\right) \qquad (9)$$

$E_{11}{}^\circ$ is the energy change, $S_{11}{}^\circ$ is the entropy loss, and $V_{11}{}^\circ$ is the volume change associated with hydrogen bond formation.

In the polymer–CDFM systems, hydrogen bond parameters were approximated as those for the poly(propylene oxide) (PPO)–chloroform system since values were not available for the polymer–CDFM systems. Of all systems characterized for HB parameters, PPO–chloroform is most similar to the experimental systems studied here. Like CDFM, chloroform is a polar chlorinated solvent capable of hydrogen bonding to the oxygen of PPO, similar to the interactions in the ester polymer–CDFM systems. The chloroform–PPO values are $E^\circ = -11.44 \times 10^6$ J/kmol, $S^\circ = -9.74 \times 10^3$ J/kmol-K, and $V^\circ = -0.85 \times 10^{-3}$ m^3/kmol.[28]

The chemical potential expressions for the LF[37] and HB[28] models are given by Sanchez. If hydrogen bonding is absent, then the hydrogen bond contribution to the total chemical potential is zero and the chemical potential reduces to that of the lattice fluid model. Equilibrium between two phases in a binary mixture exhibiting liquid–liquid equilibria is determined by the equality of the chemical potentials for each component in each phase. The equilibrium binodal and spinodal concentrations in each phase were determined using an algorithm based on the graphical method suggested by Sanchez and La-

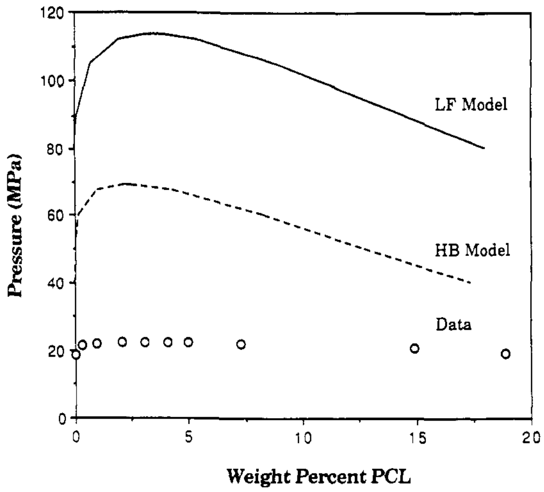

Figure 10. LF and HB predictions for PCL–CDFM (M_w = 14 600). Curves were calculated using $\zeta = 1.0$ and $\delta = 0.0$; HB curve was calculated using parameters for chloroform–PPO.

combe.[34] The accuracy of the algorithm was established by reproducing the methane–n-butane modeling results of Sanchez and Lacombe.[34]

Modeling Results. Figure 10 shows the LF modeling results for the 14 600 molecular weight PCL–CDFM system without using adjustable parameters (i.e., using $\delta = 0$ and $\zeta = 1$). LCST phase behavior was predicted. The experimental 110 °C P–x isotherm was overpredicted by about 400% using the LF model, and the shape of the predicted curve showed a much steeper dependence on the concentration than was observed experimentally. Similar results were found for the 40 500 PCL, the monodisperse PMMA, and the PE–n-alkane solutions.

Other pure component polymer scaling parameters were also used in an attempt to model the experimental data (PCL:[39] $T^* = 708$ K, $P^* = 388$ MPa, $\rho^* = 1127$ kg/m^3; PMMA:[40] $T^* = 728$ K, $P^* = 503$ MPa, $\rho^* = 1260$ kg/m^3). These parameters resulted in a larger overprediction of the experimental maximum pressure, and the slopes of the curves were more steep than for the values used in this study.

Figure 10 also shows the HB description of the experimental 14 600 molecular weight PCL–CDFM system without using adjustable parameters (i.e., using $\delta = 0$, $\zeta = 1$, and HB parameters for chloroform–PPO). Use of the HB model improved the predictions compared to the LF model, but the experimental curve was still overpredicted by about 200% and the slope and critical concentration were still not correctly described.

The flatness of the experimental isotherms could only be described using temperature-dependent parameters, with extremely large values of δ. However, under these conditions, the concentration range of predictability was severely limited, as the behavior at concentrations greater than about 5% could not be described.[41] Other mean-field theories[22,42] are also known to predict T–x curves that are much steeper than those observed experimentally.

The maximum pressure for the PCL–CDFM isotherms could not be predicted without treating δ as an adjustable parameter. For example, the best fit of the maximum pressure for the 110 °C curve was overpredicted by about 50% using $\zeta = 1.20$ and $\delta = 0$. Figure 6 shows the best fit of the experimental 14 600 molecular weight PCL–CDFM P–x isotherms using the LF model. The values of $\zeta = 1.110$ and $\delta = 0.2068$ were chosen to correctly describe the maximum experimental pressure for the 110 °C isotherm and to minimize the value of δ. Using the LF parameters fit for the 110 °C isotherm, the maximum pressures for the 70 and 140 °C isotherms were correctly described (see Figure 6), thus predicting LCST phase behavior for this system. The slope of the predicted curves, however, showed a steeper concentration dependence than was experimentally observed.

Figure 7 shows the LF prediction of the 40 500 molecular weight PCL–CDFM isotherms using the same parameters that were fit for the 14 600 PCL–CDFM 110 °C isotherm. The LF model correctly captured the molecular weight and temperature dependence of the experimental data using a single set of LF parameters. According to the LF theory, the molecular weight dependence is independent of the values used for the adjustable LF parameters δ and ζ (e.g., see eqs 2 and 3 and the expression for the chemical potential).

Using alternate PCL parameters of Rodgers and Sanchez,[39] similar results were obtained for the correct scaling of temperature and molecular weight using $\zeta = 1.050$ and $\delta = 0.2543$; however, the predicted curves showed a steeper concentration dependence than observed for the curves shown in Figures 6 and 7.

Figure 8 shows the best fit of the monodisperse PMMA–CDFM experimental isotherms using the LF model. LCST behavior was also predicted for this solution. Values of $\zeta = 0.980$ and $\delta = 0.5983$ were chosen to correctly describe the maximum experimental pressure for the 110 °C isotherm and to minimize δ. As was observed for PCL, the experimental maximum pressures could not be described without treating δ as adjustable. The temperature dependence of the experimental maximum pressures was qualitatively captured over a range of 70–140 °C using the same parameters that were fit for the 110 °C isotherm. As was seen with PCL, the predicted curves exhibited a much steeper concentration dependence than was experimentally observed.

The LF description of the PMMA solutions required a smaller value of ζ as compared to the PCL value of $\zeta = 1.110$, while larger δ values were needed for PMMA. This has its origin in the pure component parameters of PMMA and PCL given in Table II. PMMA and PCL were expected to exhibit similar solubility in CDFM as was experimentally observed since they had similar P^* values which is defined as the cohesive energy density (CED) of the fluid and is a measure of the strength of the intermolecular interactions or the "cohesiveness" of the fluid. The CED is the square of the Hildebrand solubility parameter; thus PMMA and PCL should exhibit similar solubility in CDFM, as observed experimentally. However, the T^* value (or ϵ^*) for PMMA is much larger than the T^* value for PCL (Table II), showing that PMMA exhibits stronger mer–mer interactions than PCL. As a result, the model overpredicted the P–x curves by a greater amount and predicted a steeper slope for PMMA than for PCL when using no adjustable parameters. Thus, smaller ζ and larger δ values were needed to correctly describe the experimental maximum pressures.

The experimental polyethylene–propane data of Condo et al.[19] and the experimental polyethylene–n-pentane data of Kiran and Zhuang,[14] which do not exhibit strong polar interactions, were also modeled using the LF theory. The pure component parameters used for the polyethylene, propane, and n-pentane are shown in Table II.

Figure 11 shows the modeling results for the PE–alkane systems without using adjustable parameters. The LF model predicted LCST behavior in all cases. As was noticed for the PCL and PMMA in CDFM, the experimental data were substantially overpredicted and the model curves were too steep. The best fit of Kiran's 16 400

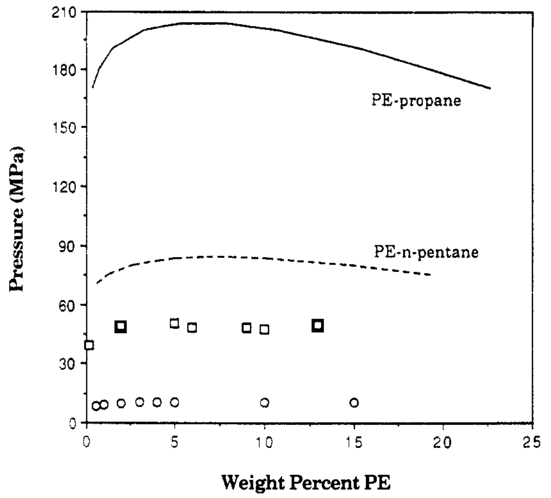

Figure 11. LF prediction of PE–n-alkane systems: (□) PE–propane, M_w = 13 600, 125 °C; (○) PE–n-pentane, M_w = 16 400, 187 °C; curves are LF predictions using ζ = 1.0 and δ 0.0.

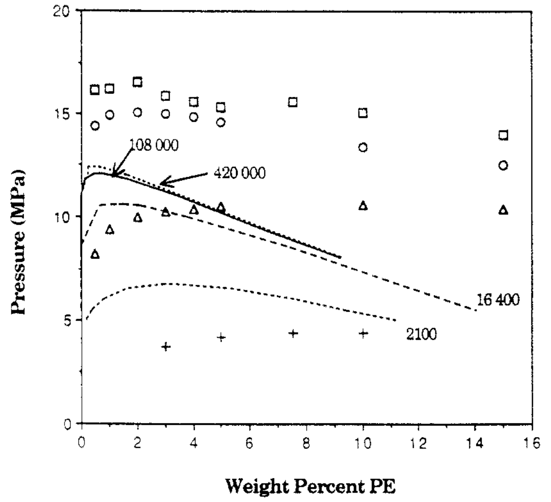

Figure 12. LF prediction of PE–n-pentane at 187 °C: (□) M_w = 420 000; (○) M_w = 108 000; (△) M_w = 16 400; (+) M_w = 2100; curves are LF predictions using ζ = 1.100 and δ = 0.2147.

molecular weight PE (M_w/M_n = 1.16) in n-pentane at 187 °C is shown in Figure 12 using ζ = 1.100 and δ = 0.2147. As was noticed for PCL and PMMA, the experimental maximum pressure could not be predicted without adjusting δ. Using the same parameters fit for the 16 400 molecular weight PE, the LF model qualitatively predicted the molecular weight dependence of the three other molecular weight PEs. The M_w = 420 000 (M_w/M_n = 2.7) and the M_w = 108 000 (M_w/M_n = 1.32) curves were underpredicted by about 33 and 25%, while the M_w = 2100 (M_w/M_n = 1.14) curve was overpredicted by about 60%. As was observed for the CDFM mixtures, the predicted isotherms exhibited a steeper dependence on concentration than was observed experimentally.

The best fit of the experimental PE–propane 125 °C isotherms of Condo et al. are shown in Figure 13. LCST phase behavior was predicted for this system. The experimental data could not be conclusively identified as either UCST or LCST. The experimental maximum pressure of the 13 000 molecular weight curve (M_w/M_n = 1.19) was fit using only one adjustable parameter, ζ = 1.0812 (δ = 0). The 120 000 molecular weight PE isotherm (M_w/M_n = 1.19) was predicted within 10% using the same parameters that were fit for the low molecular weight PE similar to the results seen for PCL and Kiran's PE–n-pentane isotherms.

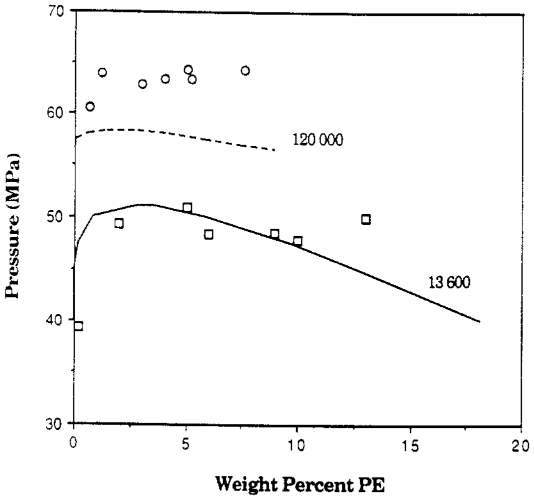

Figure 13. LF prediction of PE–propane at 125 °C: (○) M_w = 120 000; (□) M_w = 13 600; curves are LF predictions using ζ = 1.0812 and δ = 0.0.

The modeling results show that the LF theory can be used to quantitatively describe the molecular weight and temperature dependence of experimental polymer–SCF systems. However, in most cases involving SCF solvents, even for nonpolar mixtures, it is necessary to use a nonzero value for the volume mixing parameter, δ, since adjustment of the energy mixing parameter alone does not result in demixing pressures low enough to match experimental data. The δ values needed are generally large and positive—in the data treated here, δ ranged from 0 to 0.5983, while those reported by Meilchen et al. for other polymer–SCF solutions[1] ranged from 0.0015 to 0.1860.[1]

The need to use δ as an adjustable parameter in SCF solutions is not surprising, since δ allows for deviations from simple volume additivity in mixtures and SCF–solute mixtures are known to exhibit unusual behavior such as highly negative partial molar volumes.[43] The LF theory only accounts for dispersion interactions, so the energy mixing parameter ζ must account for all other possible interactions exhibited in the systems, including hydrogen bonding. In low molecular weight mixtures or in polymer-incompressible liquid solutions, ζ is found to be less than unity in nonpolar systems but greater than unity in polar systems.[27,34] However, in SCF systems that use δ as an adjustable parameter, this trend is not observed. In the nonpolar PE–alkane data examined here, $\zeta > 1$, while the hydrogen-bonding system of PMMA–CDFM exhibited ζ = 0.98; Meilchen et al. also found $\zeta < 1$ for a poly(methyl acrylate)–CDFM solution.[1] Thus, it is difficult to attribute physical significance to the parameters needed to describe polymer–SCF systems. This is at least partially due to the fact that the choice of δ influences the mixture interaction energy, as can be seen from eq 5.

The Sanchez–Panayiotou hydrogen bond model was used next in an attempt to improve the LF description of the polymer–CDFM experimental data. LCST phase behavior was predicted in all cases. Figure 10 shows the HB predictions for the 110 °C isotherm of the 14 600 PCL–CDFM system, using ζ = 1, δ = 0, and the HB parameters for PPO–chloroform. Analysis showed that the predicted phase behavior was insensitive to adjustment of the three hydrogen bond parameters, and no adjustment of the HB parameters could be used to correctly predict the experimental maximum pressure or the shape of the curves when using ζ = 1 and δ = 0. For example, the best fit of the experimental 110 °C PCL isotherm was found using values of $E°$ = -50×10^6 J/kmol, $S°$ = -1×10^3 J/kmol-K, and $V°$ = 0.85×10^{-3} m^3/kmol, but the maximum pressure was overpredicted by 110%. Thus, the PPO–chloroform parameters were used in modeling the experimental data and were not treated as adjustable parameters.

A better description of the experimental PCL maximum pressure was obtained with the HB model by treating the LF parameter ζ as adjustable. For example, using $\zeta = 1.180$, $\delta = 0$, and the HB parameters for chloroform–PPO, the experimental pressure was overpredicted by about only 50%. The experimental maximum pressure could not be predicted without treating the LF parameter δ as adjustable. When using both ζ and δ as adjustable, the HB model did not improve upon the predictions of the LF model for either PCL or PMMA. Due to the large values of δ needed to describe the maximum pressure, the chemical potential contribution of the LF model was 2 orders of magnitude larger than the HB term. Thus, the HB contributions were insignificant, and similar results as seen in Figures 6 and 7 for the LF model were obtained using the HB model.

In summary, the LF and HB models predicted LCST phase behavior for all systems studied, in agreement with experimental observation. The experimental maximum pressures for the PCL and PMMA systems were correctly predicted over a temperature range of 70–140 °C and the correct scaling of molecular weight was observed for the PCL and PE systems using a single set of LF parameters for each system. The models could not correctly describe the characteristic flatness of the demixing curves. However, since the flatness is characteristic of all experimentally observed demixing curves, the inability of the lattice models to describe this feature would not necessarily severely limit the usefulness of the theory for aiding in process design. For example, since a single set of LF parameters can describe both the temperature and molecular weight dependence of the maximum demixing pressures, a fractionation process might be designed with this information alone, since even if fractionation involved polymer concentrations above the critical concentration, the demixing pressure could be assumed similar to the maximum value.

Conclusions

General conclusions can be made from both the experimental cloud point studies of the polymer–CDFM systems and the modeling results using the lattice fluid and hydrogen bond models.

All the polymer–CDFM systems studied exhibited LCST phase behavior. The experimental P–x and T–x curves for these systems were relatively flat throughout the composition range studied from 0.03 to 19 wt %. The flatness was a general trend observed and was not affected by polydispersity or differences in polymer molecular weight. The polymer molecular weight had a relatively small effect on the magnitude of the experimental demixing curves. For example, at constant temperature and composition, doubling the PCL molecular weight increased the demixing curves by 10–20%. Overall, the experimental work shows that the phase behavior observed for the CDFM systems is independent of the critical state of the solvent. Similar phase behavior such as the flatness of the demixing curves, the LCST phase behavior, and the molecular weight effects was observed in both the subcritical and supercritical regions of the solvent.

The LF model predicted LCST phase behavior for all the polymer–CDFM and PE–n-alkane systems studied, in agreement with experimental observation. Without using adjustable LF parameters, the experimental P–x curves were overpredicted by at least 400%, while the slopes of the predicted curves were too steep. The experimental maximum pressures for both molecular weight PCL systems and for the PMMA system were correctly predicted over a temperature range of 70–140 °C using a single set of LF parameters for each system. Qualitatively correct scaling of molecular weight was observed for the PE–n-pentane and the PE–propane systems using a single set of LF parameters for each case. In all systems studied, however, the predicted isotherms exhibited a steeper concentration dependence than was observed experimentally.

The hydrogen bond model improved the LF predictions for the polymer–CDFM systems for the case of no adjustable LF parameters; however, the experimental curves were still overpredicted by at least 200% and the curves were too steep. The experimental maximum pressures could not be predicted using the HB model unless both LF parameters were treated as adjustable. In this case, similar results as seen for the LF model were predicted.

Because the LF model can correctly describe the type of phase behavior, the molecular weight scaling, and the temperature dependence of the maximum cloud point pressure, it is a useful tool for predicting the phase behavior of polymer–SCF solutions. The main drawbacks appear to be the inability of the theory to describe the concentration dependence of the cloud point curves, even for a monodisperse polymer, and the need to estimate the mixing rule parameters from experimental data.

Appendix. Polymer–CDFM Cloud Point Polynomial Curve Fits

Table A.I. PCL–CDFM (M_w = 14 600)

concn (wt % polymer)	equation (P, MPa; T, °C)
0.029	$P = -20.871 + 0.43397T - 6.7838 \times 10^{-4}T^2$
0.288	$P = -19.636 + 0.42290T - 4.4064 \times 10^{-4}T^2$
0.973	$P = -18.914 + 0.43503T - 5.7375 \times 10^{-4}T^2$
2.06	$P = -20.629 + 0.47439T - 7.6059 \times 10^{-4}T^2$
3.10	$P = -20.806 + 0.47302T - 7.3343 \times 10^{-4}T^2$
4.06	$P = -20.118 + 0.46526T - 7.1455 \times 10^{-4}T^2$
4.97	$P = -20.174 + 0.46303T - 6.9886 \times 10^{-4}T^2$
7.25	$P = -20.729 + 0.46978T - 7.2765 \times 10^{-4}T^2$
14.89	$P = -23.208 + 0.49300T - 8.4772 \times 10^{-4}T^2$
18.87	$P = -22.928 + 0.44778T - 6.0281 \times 10^{-4}T^2$

Table A.II. PCL–CDFM (M_w = 40 500)

concn (wt % polymer)	equation (P, MPa; T, °C)
0.031	$P = -20.927 + 0.48674T - 7.8029 \times 10^{-4}T^2$
0.308	$P = -19.729 + 0.47761T - 7.1376 \times 10^{-4}T^2$
1.00	$P = -20.096 + 0.49072T - 7.5342 \times 10^{-4}T^2$
3.07	$P = -18.227 + 0.45775T - 6.1003 \times 10^{-4}T^2$
5.05	$P = -19.114 + 0.47121T - 6.5685 \times 10^{-4}T^2$
7.24	$P = -19.939 + 0.47596T - 6.4877 \times 10^{-4}T^2$

Table A.III. PMMA–CDFM (M_w = 74 200)

concn (wt % polymer)	equation (P, MPa; T, °C)
0.030	$P = -20.369 + 0.37989T - 4.2093 \times 10^{-4}T^2$
0.311	$P = -21.274 + 0.41400T - 5.4051 \times 10^{-4}T^2$
0.983	$P = -22.489 + 0.44372T - 6.4710 \times 10^{-4}T^2$
3.11	$P = -20.804 + 0.41613T - 5.0146 \times 10^{-4}T^2$
5.07	$P = -22.873 + 0.46489T - 7.6064 \times 10^{-4}T^2$
8.26	$P = -21.010 + 0.41800T - 4.9133 \times 10^{-4}T^2$
15.42	$P = -24.096 + 0.45924T - 6.8208 \times 10^{-4}T^2$

Acknowledgment. This work was supported in part by the Procter & Gamble Co. under its University Exploratory Research Program and by the National Science Foundation under Grant No. DDM-9102435. We would also like to thank Tom Blackwood of the University of Delaware for helping with the cloud point experiments.

References and Notes

(1) Meilchen, M. A.; Hasch, B. M.; McHugh, M. A. *Macromolecules* **1991**, *24*, 4874.

(2) McHugh, M. A.; Krukonis, V. J. *Supercritical Fluid Extraction—Principles and Practice*; Butterworths: Boston, MA, 1986.

(3) Wissinger, R. G.; Paulaitis, M. E. *Ind. Eng. Chem. Res.* **1991**, *30*, 842.

(4) Wissinger, R. G. Thermodynamic Behavior of Glassy-Polymer–Carbon Dioxide Systems at Elevated Pressures. Ph.D. Dissertation, University of Delaware, 1988.

(5) Lele, A. K.; Shine, A. D. *AIChE J.* **1992**, *38*, 742.

(6) Matson, D. W.; Fulton, J. L.; Petersen, R. C.; Smith, R. D. *Ind. Eng. Chem. Res.* **1987**, *26*, 2298.

(7) Dixon, D. J.; Bodmeier, R. A.; Johnston, K. P. *AIChE J.* **1993**, *39*, 127.

(8) Schrantz, J. *Ind. Finishing* **1989** (Sep), 26.

(9) O'Sullivan, D. *Chem. Eng. News* **1992** (Jan 13), *70*, 21.

(10) Daneshvar, M.; Gulari, E. *Proceedings of the International Symposium on Supercritical Fluids*, Nice, Oct 17–19, 1988, p 51.

(11) Saraf, V. P.; Kiran, E. *Polymer* **1988**, *29*, 2061.

(12) Kiran, E.; Saraf, V. P. *Proceedings of the International Symposium on Supercritical Fluids*, Nice, Oct 17–19, 1988, p 43.

(13) Kiran, E.; Saraf, V. P.; Sen, Y. L. *Int. J. Thermophys.* **1989**, *10*, 437.

(14) Kiran, E.; Zhuang, W. *Polymer* **1992**, *33*, 5259.

(15) Irani, C. A.; Cozewith, C. *J. Appl. Polym. Sci.* **1986**, *31*, 1879.

(16) Baker, C. H.; Brown, W. B.; Gee, G.; Rowlinson, J. S.; Stubley, D.; Yeadon, R. E. *Polymer* **1962**, *3*, 215.

(17) Ehrlich, P.; Kurpen, J. J. *J. Polym. Sci., Part A* **1963**, *1*, 3217.

(18) Ehrlich, P.; Graham, E. B. *J. Polym. Sci.* **1960**, *45*, 246.

(19) Condo, P. D., Jr.; Colman, E. J.; Ehrlich, P. *Macromolecules* **1992**, *25*, 750.

(20) Ali, S. *Z. Phys. Chem.* **1983**, *137*, 13.

(21) Kumar, S. K.; Chhabria, S. P.; Reid, R. C.; Suter, U. W. *Macromolecules* **1987**, *20*, 2550.

(22) Walsh, D. J.; Dee, G. T. *Polymer* **1988**, *29*, 656.

(23) Haschets, C. W. Phase Behavior of Polymer–Supercritical Fluid Solutions. M.S. Thesis, University of Delaware, 1992.

(24) Ehrlich, P. *J. Polym. Sci., Part A* **1965**, *3*, 131.

(25) Swelheim, T.; De Swaan Arons, J.; Diepen, G. A. M. *Recueil* **1965**, *84*, 261.

(26) de Loos, Th. W.; Poot, W.; Diepen, G. A. M. *Macromolecules* **1983**, *16*, 111.

(27) Sanchez, I. C.; Lacombe, R. H. *Macromolecules* **1978**, *11*, 1145.

(28) Panayiotou, C.; Sanchez, I. C. *J. Phys. Chem.* **1991**, *95*, 10090.

(29) Gupta, R. B.; Panayiotou, C. G.; Sanchez, I. C.; Johnston, K. P. *AIChE J.* **1992**, *38*, 1243.

(30) Altunin, V. V.; Geller, V. Z.; Petrov, E. K.; Rasskazov, D. C.; Spiridonov, G. A. *Thermophysical Properties of Freons, Methane Series, Part I*; Hemisphere: Washington, DC, 1987.

(31) McHugh, M. A. An Experimental Investigation of the High Pressure Fluid Phase Equilibria of Highly Asymmetric Binary Mixtures. Ph.D. Dissertation, University of Delaware, 1981.

(32) Kwei, T. K. In *Macromolecules*; Bovey, F. A., Winslow, F. H., Eds.; Academic Press: New York, 1979; p 273.

(33) Leibler, L. In *Encyclopedia of Polymer Science and Engineering*; Mark, H. F., Ed.; Wiley: New York, 1988; Vol. 11, p 30.

(34) Lacombe, R. H.; Sanchez, I. C. *J. Phys. Chem.* **1976**, *80*, 2568.

(35) Panayiotou, C. G. *Macromolecules* **1987**, *20*, 861.

(36) Sanchez, I. C.; Lacombe, R. H. *J. Phys. Chem.* **1976**, *80*, 2352.

(37) Sanchez, I. C. *J. Macromol. Sci., Phys.* **1980**, *B17*, 565.

(38) Lambert, J. D.; Clarke, J. S.; Duke, J. F.; Hicks, C. L.; Lawrence, S. D.; Morris, D. M.; Shone, M. G. T. *Proc. R. Soc. London* **1959**, *249A*, 414.

(39) Rodgers, P. A.; Sanchez, I. C. *J. Polym. Sci., Polym. Phys. Ed.* **1993**, *31*, 273.

(40) Sanchez, I. C. Personal Communication, University of Texas at Austin.

(41) Haschets, C. W.; Blackwood, T. A.; Shine, A. D. *Polym. Prepr. (Am. Chem. Soc., Div. Polym. Chem.)* **1993**, *34* (1), 602.

(42) Shultz, A. R.; Flory, P. J. *J. Am. Chem. Soc.* **1952**, *74*, 4760.

(43) Eckert, C. A.; Ziger, D. H.; Johnston, K. P.; Ellison, T. K. *Fluid Phase Equilibria* **1983**, *14*, 167.

Author Supplied Registry Nos. Chlorodifluoromethane, 75-45-6; propane, 74-98-6; *n*-pentane, 109-66-0; polyethylene, 9002-88-4; poly(methyl methacrylate), 9011-14-7; polycaprolactone, 24980-41-4.